Immunonanoshells for targeted photothermal ablation of tumor cells

Amanda R Lowery[1]
André M Gobin[1]
Emily S Day[1]
Naomi J Halas[2]
Jennifer L West[1]

[1]Department of Bioengineering, [2]Department of Electrical and Computer Engineering, Rice University, Houston, TX, USA

Abstract: Consisting of a silica core surrounded by a thin gold shell, nanoshells possess an optical tunability that spans the visible to the near infrared (NIR) region, a region where light penetrates tissues deeply. Conjugated with tumor-specific antibodies, NIR-absorbing immunonanoshells can preferentially bind to tumor cells. NIR light then heats the bound nanoshells, thus destroying the targeted cells. Antibodies can be consistently bound to the nanoshells via a bifunctional polyethylene glycol (PEG) linker at a density of ~150 antibodies per nanoshell. In vitro studies have confirmed the ability to selectively induce cell death with the photothermal interaction of immunonanoshells and NIR light. Prior to incubation with anti-human epidermal growth factor receptor (HER2) immunonanoshells, HER2-expressing SK-BR-3 breast carcinoma cells were seeded alone or adjacent to human dermal fibroblasts (HDFs). Anti-HER2 immunonanoshells bound to HER2-expressing cells resulted in the death of SK-BR-3 cells after NIR exposure only within the irradiated area, while HDFs remained viable after similar treatment since the immunonanoshells did not bind to these cells at high levels. Control nanoshells, conjugated with nonspecific anti-IgG or PEG, did not bind to either cell type, and cells continued to be viable after treatment with these control nanoshells and NIR irradiation.

Keywords: nanoshells, immunonanoshells, photothermal, antibody, targeting, cancer

Introduction

Metal nanoshells are optically tunable nanoparticles, consisting of a spherical dielectric core encapsulated by a thin metal shell. The overall particle size as well as the ratio of core radius to shell thickness dictates the scattering and absorbing properties of the particle. For a given core radius, decreasing the shell thickness (increasing the core: shell ratio) shifts the peak plasmon resonance to longer wavelengths (Oldenburg et al 1998; Averitt et al 1999). The resonance tunablity spans the visible and infrared spectrum (Averitt et al 1999). By placing the peak absorption properties in the near infrared (NIR) region where tissue absorption is at a minimum (Welch and van Gemert 1995; Weissleder 2001), nanoshells within tissue can preferentially absorb NIR light energy.

Nanoshell photothermal cancer therapy works through the preferential accumulation of nanoshells in a tumor and absorption of NIR light by those particles to locally generate heat at the tumor site. Nanoshells have been shown to passively accumulate in tumors after intravenous injection (O'Neal et al 2004) as a result of the leaky vasculature characteristic of neoplastic tumors (Hashizume et al 2000). After systemic injection and accumulation at the tumor site, NIR light is applied over the tumor region. The absorbed energy causes the nanoshells to heat, allowing local destruction of the tumor tissue. In a mouse model, nanoshell-treated tumors completely regressed after NIR illumination without tumor regrowth (O'Neal et al 2004). The tumors receiving

Correspondence: Jennifer L West
Rice University, MS 142, 6100 Main Street, Houston, TX 77005, USA
Tel +1 713 348 5955
Fax +1 713 348 5154
Email jwest@rice.edu

the nanoshell therapy experienced rapid temperature rises sufficient to cause irreversible tissue damage, while laser application to nearby healthy tissue or to tumors not treated with nanoshells did not induce a significant temperature increase (Hirsch et al 2003).

Molecularly targeting nanoshells to tumors via antibodies against cell surface markers may further enhance the accumulation of nanoshells in tumors, prolong their presence in tumors, and potentially allow the use of lower nanoshell dosages. Many tumors have increased expression of specific cell surface markers. Several markers have been investigated for targeting applications, including human epidermal growth factor receptor (HER2) (Wu et al 2003), α_v integrin (Arap et al 1998; Anderson et al 2000; Reynolds et al 2003), and CD44 (Verel et al 2002). These targets have been used to deliver genes (Reynolds et al 2003), chemotherapeutics (Backer and Backer 2001), and nanoparticles (Anderson et al 2000; Wu et al 2003). Antibody targeting of nanoparticles and drugs to tumors has shown increased delivery of therapeutic agents (Tarli et al 1999; Cortez-Retamozo et al 2002; Reynolds et al 2003). Specifically, the human epidermal growth factor receptor HER2 has been used to target breast cancer cells because of its stable overexpression on ~30% of breast cancers (Slamon et al 1989; McDermont et al 2002; Kämmerer et al 2003; Carlsson et al 2004). Using HER2 targeted immunoliposomes, the uptake of the chemotherapeutic drug doxorubicin was increased 700-fold (Park et al 2001, 2002; Noble et al 2004). In the current studies, antibody conjugation to nanoshells has been evaluated, and nanoshells conjugated with anti-HER2 are investigated for targeting nanoshell binding to HER2-expressing breast carcinoma cells.

Materials and methods

Synthesis of polyethylene (PEG) thiol (PEG-SH)

PEG-SH was synthesized by reacting PEG-amine (M_r 5000, Nektar, Huntsville, AL, USA) with 2-iminothiolane (Sigma-Aldrich, St Louis, MO, USA) for 1 hour. The product was dialyzed (molecular weight cutoff of 500 Da; Spectrum Laboratories, Rancho Domingo, CA, USA) against deionized (DI) water for at least 4 hours to remove excess reagents. The PEG-SH yield was determined colorimetrically at 412 nm after reacting with Ellman's reagent, 5,5'-dithio-bis(2-nitrobenzoic acid) (Sigma-Aldrich). PEG-SH was stored at –20°C.

Antibody PEG conjugation

Orthopyridyl-disulfide-poly(ethylene glycol)-N-hydroxysuccinimide ester (OPSS-PEG-NHS, 2000 Da) was obtained from Nektar (San Carlos, CA, USA) in lyophilized form. C-*erb*B-2/HER2/*neu* Ab-4 (clone N12) (anti-HER2) was obtained from NeoMarkers (Fremont, CA, USA). A 81 µmol/L (0.16 mg/mL) solution of OPSS-PEG-NHS was mixed with 5.4 µmol/L (1 mg/mL) anti-HER2 at a volumetric ratio of 1:9 and reacted at 4°C overnight.

Nanoshell synthesis

Nanoshells were synthesized as previously described (Oldenburg et al 1998; Averitt et al 1999). Briefly, silica nanoparticles were fabricated by the Stöber method (Stöber et al 1968) in which tetraethyl orthosilicate is reduced in basic ethanol. The surfaces of the silica particles were reacted with aminopropyl triethoxysilane, terminating the surface with amine groups. Small gold colloid (~3 nm), prepared by the method of Duff et al (1993), was then adsorbed onto the nanoparticle surface. The adsorbed colloid was used as nucleation sites for reduction of additional gold onto the surface to generate a contiguous shell of gold. Nanoshells were evaluated by their optical absorption profiles using a Cary 50 BIO UV Vis spectrophotometer and size distribution under scanning electron microscopy (XL30, Philips Electron Optics, Netherlands). The nanoshells used in the following study had a 110 nm core diameter with an 11 nm thick gold shell and peak extinction at ~820 nm.

Nanoshell anti-HER2 conjugation

PEG-conjugated anti-HER2/*neu* (0.9 mg/mL) was added to 8.8×10^8 nanoparticles/ml (absorption=1.5 at 800 nm at 1 cm path length) to obtain a final antibody concentration of 7.5 µg/mL. The suspension was reacted at 4°C overnight. A 0.05 mM PEG-SH solution was added to the nanoshells at a volume ratio of 9 parts nanoshells:1 part PEG-SH and reacted at 4°C overnight. Immunonanoshells were divided as 1 mL aliquots into 2.0 mL eppendorf tubes (Sigma-Aldrich). The aliquots were centrifuged at 500 *g* for 5 min (Eppendorf Centrifuge 5415C). Immediately, the supernatant was removed and aliquots were resuspended in McCoy's 5a medium supplemented with 10% fetal bovine serum (FBS), 1.8 mM L-glutamine, 90 units/mL penicillin, and 0.9 µg/mL streptomycin to obtain a final nanoshell concentration of 2.9×10^9 particles/mL (absorption = 5 at 800 nm at a 1 cm path length).

Quantification of the number of antibodies per nanoshell (ELISA)

Immunonanoshells were incubated with horseradish peroxidase-labeled (HRP) anti-mouse IgG (Sigma-Aldrich, A3682) for 1 hour. Nonspecific reaction sites were blocked with a 3% solution of bovine serum albumin (BSA). Nanoshells were rinsed to remove any unbound IgG. The HRP bound to the immunonanoshells was reacted with 3,3',5,5'-tetramethylbenzidine to generate a colored product and compared with a HRP anti-mouse IgG standard curve ranging from $7x10^{-6}$ to $7x10^{-9}$g/ml. Results were read using a spectrophotometer (Cary BIO 50, Varian, CA, USA) at 450 nm.

Imaging of antibodies bound to nanoshells

Immunonanoshells, prepared as described above, were incubated with gold-labeled anti-mouse IgG (Molecular Probes, Eugene, OR, USA) for 1 hour. Nonspecific reaction sites were blocked with a 3% solution of BSA. Nanoshells were rinsed to remove any unbound IgG. Samples were mounted on copper grids and imaged with a JEOL 2010 transmission electron microscope (TEM, JEOL Ltd., Japan).

Cell maintenance

Chemicals were obtained from Sigma-Aldrich unless otherwise stated. SK-BR-3 breast carcinoma cells were obtained from American Type Culture Collection (ATCC, Manassas, VA, USA). Cells were maintained in McCoy's 5a medium supplemented with 10% FBS, 1.8 mM L-glutamine, 90 units/mL penicillin, and 0.9 µg/mL streptomycin. MCF-7 breast carcinoma cells (HER2 negative) were obtained from ATCC and maintained in Eagle's Minimal Essential Medium supplemented with 10% FBS, 1.8 mM L-glutamine, 90 units/mL penicillin, 0.9 µg/mL streptomycin, and 0.01 mg/mL bovine insulin. Human dermal fibroblasts (HDFs) were obtained from ATCC and maintained in Dulbecco's Modified Eagle's Medium (DMEM) supplemented with 10% FBS, 1.8 mM L-glutamine, 90 units/ml penicillin, and 0.9 µg/ml streptomycin. Cells were incubated at 37°C in a 5% CO_2 environment. For monoculture experiments, cell were seeded into 24-well trays at $1x10^4$ cells/cm^2 and cultured to near confluency. For side-by-side co-culture experiments, where 2 cell types were located adjacent to one another, each cell type was grown separately on glass cover slips coated in 1% gelatin. Immediately prior to nanoshell incubation, 2 cover slips containing different cell types were aligned such that the cover slips set side-by-side on a glass-chambered slide without a gap separating them.

Photothermal destruction of cells incubated with immunonanoshells

Cells were rinsed 3 times in phosphate buffered saline (PBS, pH 7.4). Nanoshells were mixed with 10x McCoy's 5A medium without FBS at a ratio of 9:1. 500 µl of nanoshell suspension was added to the cell cultures. Cells were returned to the 37°C incubator for 45 minutes. Following incubation, cells were rinsed 3 times in PBS and then covered in McCoy's 5A medium. Cells were exposed to NIR laser irradiation (Coherent, 820 nm, 0.8 W/m^2 for 7 min) and then returned to the 37°C incubator overnight.

Silver staining to evaluate nanoshell binding

Cells were fixed with a 2.5% formalin solution for 10 minutes then rinsed 3 times with DI water. A silver staining kit (Amersham Biosciences, Piscataway, NJ, USA) was used to stain cells, depositing silver onto the gold nanoshell surfaces, to allow visualization of nanoshell binding to cells via light microscopy.

Viability staining

A Live/Dead Stain Kit (calcein AM and ethidium homodimer, Molecular Probes, CA, USA) was used to evaluate cell viability after NIR treatment. Cells were then examined by fluorescence microscopy (Ziess Axiovert 135, Thornwood, NY, USA).

Results

Quantification and imaging of antibodies on nanoshells

The anti-HER2 conjugated nanoshells bound a significant number of antibodies compared with PEG-coated nanoshells ($p<0.05$). Each immunonanoshell was conjugated with 152±128 anti-HER2 antibodies. The ELISA-style assay confirmed that no antibodies were present on the nanoshells coated with PEG only (–16±19 antibodies/nanoshell). In the TEM image of the nanoshell (Figure 1), the binding of the gold colloid-labeled secondary antibody can be clearly seen. Additionally, the visualization of antibody conjugation is in good agreement with the quantification achieved using the ELISA-style assay.

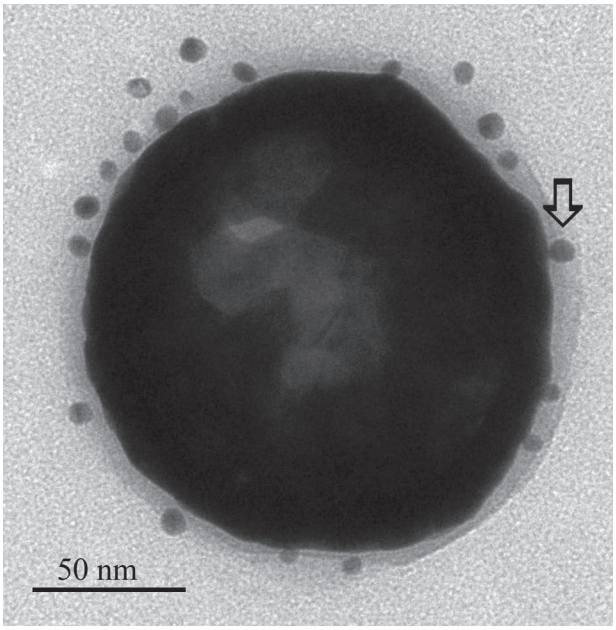

Figure 1 Transmission electron micrograph of an immunonanoshell with gold-labeled antibodies (example indicated by arrow) shows several antibodies bound to the nanoshell surface within the hazy polyethylene glycol (PEG) layer.

Photothermal destruction of mono-cultured cells incubated with immunonanoshells

Anti-HER2 conjugated nanoshells associated specifically with HER2 expressing cells at sufficient concentrations such that the combination of nanoshells and NIR light-induced cell death. Anti-HER2 conjugated nanoshells bound to the SK-BR-3 cell surface, as seen in the silver stain image (Figure 2f), and induced cell death within the laser exposure area, as seen in the viability stain (Figure 2c). Incubation of SK-BR-3 cells with nanoshells conjugated with a non-specific anti-IgG (Figure 2a, d) or with PEG alone (Figure 2b, e) did not facilitate the binding of the nanoshells to the cell surface. Anti-HER2 conjugated nanoshells did not bind to MCF-7 cells, which do not express HER2.

Photothermal destruction of targeted cells in co-culture

In Figure 3, where the two cell types were adjacent to one another, only cells within the laser spot and of the targeted cell type were destroyed by the treatment. The HDFs, also exposed to the NIR light, did not die. When co-cultures were incubated with PEG-coated nanoshells (Figure 3b), both cell types remained viable after laser irradiation. Only the HER2-expressing SK-BR-3 cells bound with anti-HER2 immunonanoshells and irradiated with NIR laser died.

Discussion

The anti-HER2 conjugated nanoshells bound a significant number of antibodies. The density of ~152 anti-HER2 antibodies per immunonanoshell exceeded that obtained on immunoliposomes of similar size, where 30–50 antibodies per liposome were achieved (Cerletti et al 2000; Park et al 2002). The ELISA-style data are supported by the TEM images (Figure 1) where the gold-labeled secondary antibody bound to the anti-HER2 antibody speckles the outer surface of the conjugated nanoshell. TEM imaging and the ELISA

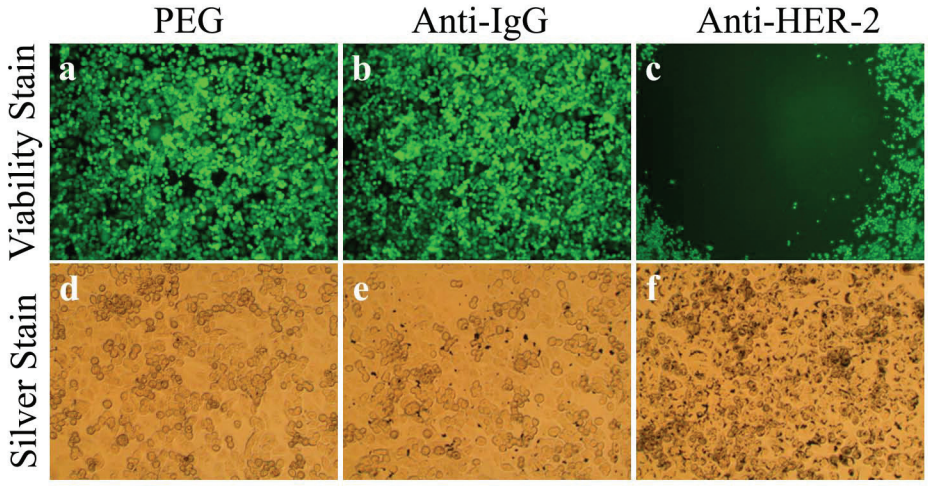

Figure 2 Antibody conjugated nanoshells bound to cells when the appropriate antigen was present. SK-BR-3 cells were incubated with PEG-coated nanoshells (a, d), anti-IgG conjugated nanoshells (b, e), and anti-HER2 conjugated nanoshells (c, f). Following laser exposure, a region of cell death corresponding to the laser spot resulted in groups incubated with anti-HER2 conjugated nanoshells (c). Cells incubated with PEGylated or anti-IgG conjugated nanoshells continued to live. Silver staining (d–f) showed maximal binding of anti-HER2 conjugated nanoshells to the SK-BR-3 cells (f). Laser spot is 1.5 mm wide.
Abbreviations: HER2, epidermal growth factor receptor; PEG, polyethylene glycol.

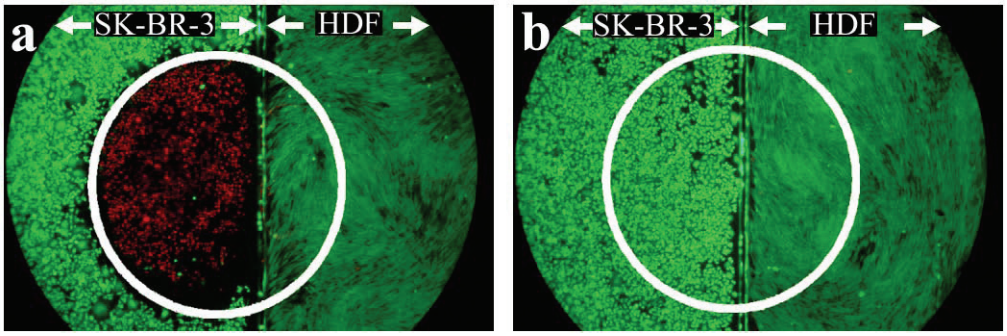

Figure 3 Two cell types, SK-BR-3 (left side of a and b) and HDF (right side of a and b) cells, were grown on glass cover slip and aligned as shown prior to the experiment. (a) Anti-HER2 immunonanoshells bound to the HER2 expressing SK-BR-3 cells resulted in targeted cell death after laser irradiation. The laser area is outlined in white. (b) Nanoshells coated in PEG only did not bind cells and laser irradiation produced no area of cell death. Laser spot is 2.5 mm wide.
Abbreviations: HDF, human dermal fibroblasts; HER2, epidermal growth factor receptor; PEG, polyethylene glycol.

assay confirmed that no antibodies were present on the nanoshells coated with PEG only.

Anti-HER2 conjugated immunonanoshells bound to the SK-BR-3 cell surface and induced cell death within the laser exposure area. Anti-HER2 nanoshells did not bind to MCF-7 cells, which do not express HER2. Incubation of SK-BR-3 cells with nanoshells conjugated with a nonspecific anti-IgG or with PEG alone did not facilitate the binding of the nanoshells to the cell surface. As previously seen, cell death requires the simultaneous exposure of cells to both nanoshells and NIR light (Hirsch et al 2003; Loo et al 2004, 2005). Nonspecific anti-IgG nanoshells and PEG nanoshells, not bound to cell surfaces, were rinsed away during washing thus preventing cell death after NIR irradiation.

The cellular specificity of the nanoshell treatment achieved through the addition of the antibody was verified in the co-culture experiments. In Figure 3, where the SK-BR-3 cells and HDFs were adjacent to one another, only cells within the laser spot and of the targeted cell type died. NIR light was applied to the co-culture overlapping both cell types simultaneously. An area of cell death resulted only on the targeted SK-BR-3 cells incubated with anti-HER2 immunonanoshells. When co-cultures were incubated with PEG-coated nanoshells, both cell types continued to live after laser irradiation. Only the HER2-expressing cells bound with anti-HER2 immunonanoshells and irradiated with the NIR laser died, even when they were in close proximity to nontargeted healthy cells.

The in vitro studies detailed here demonstrate the ability of the immunonanoshells to bind specifically and to facilitate the thermal therapy locally on an individual cell level. Within tumors, the active binding of nanoshells will increase the accumulation by promoting longer retention times in the tumor. The incorporation of an antibody onto the nanoshell surface should increase the uptake within targeted tissues in vivo.

Conclusions

The addition of a tumor-specific antibody should increase the specificity of the nanoshell therapy, as indicated by these initial in vitro results. Immunonanoshells bind to targeted cells whether the cells are alone or adjacent to healthy cells. Upon laser irradiation, the cells bound by nanoshells are killed, leaving the healthy cells unharmed. Successful treatments not only require the laser and nanoshells to be present simultaneously, but in order for nanoshells to be present in vitro, they must actively bind to the targeted cell type. In vivo, the accumulation of immunonanoshells within a tumor will not simply rely on the enhanced permeability of tumors as previously demonstrated (O'Neal et al 2004). In addition to utilizing the elevated permeability of tumors, the ability of immunonanoshells to bind tumor cells should further promote the localization of nanoshells within the tumor. The increased specificity by the antibodies has tailored the immunonanoshell for higher accumulations at targeted tissues and thus improved the nanoshell therapeutic efficiency.

Acknowledgments

We would like to acknowledge Karl Krueger for his help with collecting the TEM images. Funding for this project was provided by the Department of Defense, a National Institutes of Health training grant, and a training fellowship from the Keck Center Nanobiology Training Program of the Gulf Coast Consortia, NIH Grant No.1 T90 DK070121-01 (US citizens/permanent residents).

References

Anderson SA, Rader RK, Westlin WF, et al. 2000. Magnetic resonance contrast enhancement of neovasculature with αvβ3-targeted nanoparticles. *Magn Reson Med*, 44:433–9.

Arap W, Pasqualini R, Ruoslahti E. 1998. Cancer treatment by targeted drug delivery to tumor vasculature in a mouse model. *Science Magazine*, 16:377–80.

Averitt RD, Westcott SL, Halas NJ. 1999. Linear optical properties of gold nanoshells. *J Opt Soc Am B*, 16:1824–32.

Backer MV, Backer JM. 2001. Targeting endothelial cells overexpressing VEGFR-2: Selective toxicity of shiga-like toxin-VEGF fusion proteins. *Bioconjug Chem*, 12:1066–73.

Carlsson J, Nordgren H, Sjostrom J, et al. 2004. HER2 expression in breast cancer primary tumours and corresponding metastases. Original data and literature review. *Br J Cancer*, 90:2344–8.

Cerletti A, Drewe J, Fricker G, et al. 2000. Endocytosis and transcytosis of an immunoliposome-based brain drug delivery system. *J Drug Target*, 8:435–46.

Cortez-Retamozo V, Lauwereys M, Hassanzadeh G, et al. 2002. Efficient tumor targeting by single-domain antibody fragments of camels. *Int J Cancer*, 98:456–62.

Duff DG, Baiker A, Edwards P. 1993. A new hydrosol of gold clusters. 1. Formation and particle size variation. *Langmuir*, 9:2301–9.

Hashizume H, Baluk P, Morikawa S, et al. 2000. Openings between defective endothelial cells explain tumor vessel leakiness. *Am J Pathol*, 156:1363–80.

Hirsch LR, Stafford RJ, Bankson JA, et al. 2003. Nanoshell-mediated near-infrared thermal therapy of tumors under magnetic resonance guidance. *Proc Natl Acad Sci U S A*, 100:13549–54.

Kämmerer U, Thanner F, Kapp M, et al. 2003. Expression of tumor markers on breast and ovarian cancer cell lines. *Anticancer Res*, 23:1051–6.

Loo C, Lin A, Hirsch L, et al. 2004. Nanoshell-enabled photonics-based imaging and therapy of cancer. *Technol Cancer Res Treat*, 3:33–40.

Loo C, Lowery A, Halas N, et al. 2005. Immunotargeted nanoshells for integrated cancer imaging and therapy. *Nano Lett*, 5:709–11.

McDermont RS, Beuvon F, Pauly M, et al. 2002–03. Tumor antigens and antigen-presenting capacity in breast cancer. *Pathobiology*, 70:324–32.

Noble CO, Kirpotin DB, Hayes ME, et al. 2004. Development of ligand-targeted liposomes for cancer therapy. *Expert Opin Ther Targets*, 8:335–53.

Oldenburg SJ, Averitt RD, Westcott SL, et al. 1998. Nanoengineering of optical resonances. *Chem Phys Lett*, 288:243–7.

O'Neal DP, Hirsch LR, Halas NJ, et al. 2004. Photo-thermal tumor ablation in mice using near infrared-absorbing nanoparticles. *Cancer Lett*, 209:171–6.

Park JW, Hong K, Kirpotin DB, et al. 2002. Anti-HER2 immunoliposomes: enhanced efficacy attributable to targeted delivery. *Clin Cancer Res*, 8:1172–81.

Park JW, Kirpotin DB, Hong K, et al. 2001. Tumor targeting using anti-her2 immunoliposomes. *J Control Release*, 74:95–113.

Reynolds AR, Moghimi SM, Hodivala-Dilke K. 2003. Nanoparticle-mediated gene delivery to tumor neovasculature. *Trend Mol Med*, 9:2–4.

Slamon DJ, Godolphin W, Jones LA, et al. 1989. Studies of the HER-2/neu proto-oncogene in human breast and ovarian cancer. *Science*, 244:707–12.

Stöber W, Fink A, Bohn E. 1968. Controlled growth of monodisperse silica spheres in the micron size range. *J Colloid Interface Sci*, 26:62–9.

Tarli L, Balza E, Viti F, et al. 1999. A high affinity human antibody that targets tumoral blood vessels. *Blood*, 94:192–8.

Verel I, Heider K-H, Siegmund M, et al. 2002. Tumor targeting properties of monoclonal antibodies with different affinity for target antigen CD44V6 in nude mice bearing head-and-neck cancer xenografts. *Int J Cancer*, 99:396–402.

Weissleder HB. 2001. A clearer vision for *in vivo* imaging. *Nat Biotechnol*, 19:316–7.

Welch A, van Gemert M (eds). 1995. Optical-thermal response of laser-irradiated tissues. New York: Plenum Press.

Wu X, Liu H, Liu J, et al. 2003. Immunofluorescent labeling of cancer marker Her2 and other cellular targets with semiconductor quantum dots. *Nat Biotechnol*, 21:41–6.